Electronic Supplementary Material (ESI) for Physical Chemistry Chemical Physics.
This journal is © the Owner Societies 2022

Electronic Supplementary Information for

"Strain tunable topological phase transition and skyrmions in Janus $MnSbBiSe_2Te_2$ monolayer"

Zebin Wu[1,2], Yufei Xue[1], Zhong Shen[1] and Changsheng Song[1,3†].

[1]Key Laboratory of Optical Field Manipulation of Zhejiang Province, Department of Physics, Zhejiang Sci-Tech University, Hangzhou 310018, China.

[2]School of Physics, University of Electronic Science and Technology of China, Chengdu 611731, China.

[3]Longgang Institute of Zhejiang Sci-Tech University, Wenzhou 325802, China.

[†]Email: cssong@zstu.edu.cn

I. Heisenberg exchange interactions *J*, effective magnetic anisotropy energy E_{eff} and Dzyaloshinskii-Moriya interaction $\vec{D}_{ij}$.

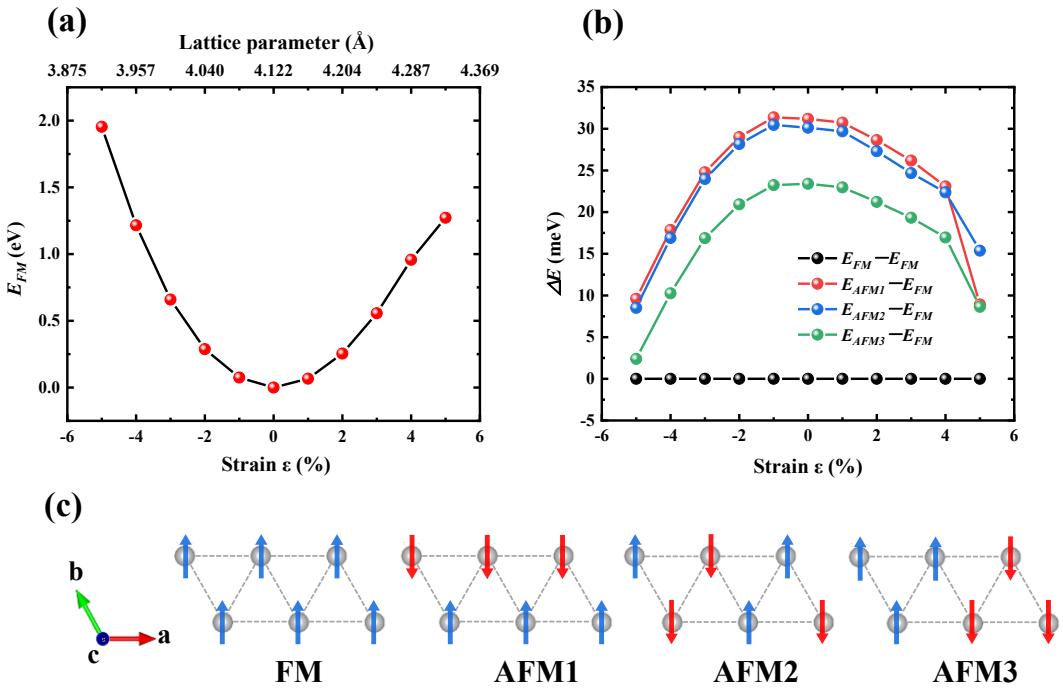

Fig. S1. (a) The FM state energy variations as a function of the lattice parameter or biaxial strain ε. (b) The relationship between relative total energy of different spin configurations and strain ε (E_{FM} is set to zero). (c) Schematic top view of four possible magnetic configurations. Red and blue arrows represent spin-up and spin-down, respectively.

To acquire Heisenberg exchange interactions *J*, we build a 3 × 2 × 1 supercell and calculate the energies of four possible magnetic configurations shown in Fig. S1(c). The total energy expressions can be described by Eq (1) in the main text as follows:

$$E_{FM} = E_0 - (18J_1 + 18J_2 + 18J_3)\,S^2, \quad \text{(S1)}$$

$$E_{AFM1} = E_0 - (-6J_1 - 6J_2 + 18J_3)\,S^2, \quad \text{(S2)}$$

$$E_{AFM2} = E_0 - (-6J_1 + 2J_2 + 2J_3)\,S^2, \quad \text{(S3)}$$

$$E_{AFM3} = E_0 - (-2J_1 - 6J_2 + 2J_3)\,S^2. \quad \text{(S4)}$$

Where J_1, J_2, J_3 are the Heisenberg exchange interactions of first, second and third nearest neighbors. E_0 is a constant of non-magnetic section, which is not related to the spin of magnetic atoms.

Usually, an accurate estimation of T_C requires more nearest neighbors to converge the result. Therefore, we manage to calculate the fourth nearest neighbor exchange J_4 within the same 3 × 2 × 1 supercell. Similarly, the related energy expressions are described as follows:

$$E_{FM} = E_0 - (18J_1 + 18J_2 + 18J_3 + 36J_4)\, S^2, \quad \text{(S5)}$$

$$E_{AFM1} = E_0 - (-6J_1 - 6J_2 + 18J_3 - 12J_4)\, S^2, \quad \text{(S6)}$$

$$E_{AFM2} = E_0 - (-6J_1 + 2J_2 + 2J_3 + 4J_4)\, S^2, \quad \text{(S7)}$$

$$E_{AFM3} = E_0 - (-2J_1 - 6J_2 + 2J_3 + 0J_4)\, S^2. \quad \text{(S8)}$$

The corresponding results are shown in Table SI. One can find that J_4 is only about 0.023 meV, which is consistent with the value of pristine MBT in the previous studies[**1, 2**].

Since the distance of the fourth or the further nearest neighbor Mn-Mn pair is very far away (greater than 10 Å), the energy values of them are usually found to be one or two orders of magnitude smaller than that of J_2 and J_3, which is expected to be negligible. Therefore, only the first three nearest neighbor interactions (*i.e.* J_1, J_2 and J_3) are applied in the Monte Carlo and micro-magnetic simulations in this work.

The in-plane orientation of the magnetic moments is understood by calculating the effective magnetic anisotropy energy (E_{eff}), which contains magneto crystalline anisotropy (MCA) energy (E_{MCA}) and magnetic shape anisotropy (MSA) energy (E_{MSA}), i.e., $E_{eff} = E_{MCA} + E_{MSA}$.

In calculations, E_{MCA} is defined as the total energy difference between in-plane and out-of-plane magnetizations of a 1×1 unit cell of Janus MSBST ($E_{MCA} = E_{in} - E_{out}$), while E_{MSA} ($E_{MSA} = E_{in}^{dipole} - E_{out}^{dipole}$) can be calculated based on the energy of magnetic dipole-dipole interactions as:

$$E_{MSA} = -\frac{1}{2}\frac{\mu_0 g^2 {\mu_B}^2}{4\pi} \sum_{i \neq j}^{N} \frac{1}{r_{ij}^3} \left[\vec{M}_i \cdot \vec{M}_j - \frac{3}{r_{ij}^2} \left(\vec{M}_i \cdot \vec{r}_{ij}\right)\left(\vec{M}_j \cdot \vec{r}_{ij}\right) \right]. \quad \text{(S9)}$$

Where the $\vec{M}_i$ represents the local magnetic moments and $\vec{r}_{ij}$ is the vector connecting site *i* and *j*, μ_0 is the vacuum permeability, g is the electron spin factor and μ_B is the Bohr magneton. A cutoff radius of at least 30 μm was used to calculate E_{MSA}.

Using the same method, our calculation of pristine $MnBi_2Te_4$ monolayer shows its E_{MCA} = 0.135 meV and E_{MSA} = -0.12 meV, indicating that pristine $MnBi_2Te_4$ prefers out-off plane magnetization with MAE = 0.015 meV, in agreement with the previous works[**3, 4**].

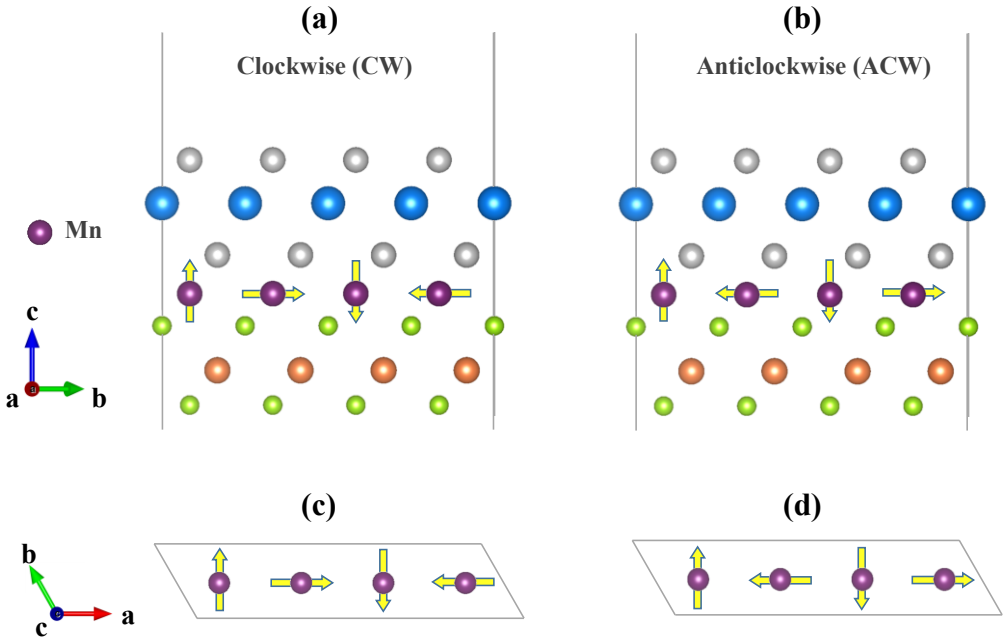

Fig. S2. Clockwise (CW) and anticlockwise (ACW) spin configurations of Janus MSBST with XZ plane (upper panel) and XY plane (lower panel), respectively.

The DMI vector $\vec{D}_{ij}$ for each pair of nearest-neighbor Mn atoms is perpendicular to their bonds, and can be expressed as:

$$\vec{D}_{ij} = d_{//}(\vec{z} \times \vec{u}_{ij}) + d_{\perp}\vec{z}, \tag{S10}$$

where the $d_{//}$ and $d_{\perp}$ are in-plane and out-of-plane component of $\vec{D}_{ij}$ vector. $\vec{z}$ and $\vec{u}_{ij}$ are unit vectors pointing along the z direction and from site i to j, respectively. By calculating the energies of clockwise (CW) and anticlockwise (ACW) spin configurations in a $4 \times 1 \times 1$ supercell with XY and XZ planes respectively, $d_{//}$ and $d_{\perp}$ can be obtained by:

$$d = (E_{ACW} - E_{CW})/12. \tag{S11}$$

Then, the strength of DMI, *i.e.,* modulus length of DMI vector can be obtained by:

$$|\vec{D}_{ij}| = D_{tot} = \sqrt{{d_{//}}^2 + {d_{\perp}}^2}. \tag{S12}$$

The corresponding results are shown in Table SI.

Table. SI Heisenberg exchange coefficients J_1, J_2, J_3, J_4, the total and two components of DMI, E_{eff} and magnetic moment of Mn atom (MAG_{Mn}) with different strains ε in Janus MSBST monolayer. All the unit of J and D parameters are in meV, and the unit of E_{eff} and MAG_{Mn} are in meV/*u.c.* and μ_B respectively.

ε (%)	J_1	J_2	J_3	J_4	D_{tot}	$D_{//}$	$D_{\perp}$	E_{eff}	MAG_{Mn}
−5	0.940	−0.371	−0.257	0.007	0.541	0.541	0.000	0.235	4.405
−4	1.083	−0.309	−0.210	0.013	0.462	0.462	0.000	0.029	4.416
−3	1.171	−0.249	−0.174	0.018	0.405	0.405	0.000	0.107	4.429
−2	1.306	−0.199	−0.150	0.022	0.371	0.371	0.000	−0.233	4.438
−1	1.423	−0.168	−0.139	0.023	0.345	0.345	0.000	−0.301	4.448
0	1.431	−0.129	−0.131	0.023	0.325	0.325	−0.002	−0.338	4.458
1	1.471	−0.139	−0.133	0.023	0.312	0.312	−0.001	−0.359	4.469
2	1.419	−0.115	−0.143	0.021	0.297	0.297	0.000	−0.364	4.477
3	1.277	−0.083	−0.132	0.019	0.286	0.286	0.000	−0.356	4.486
4	1.066	−0.117	−0.111	0.017	0.274	0.274	0.000	−0.329	4.490
5	0.764	−0.073	−0.093	0.007	0.260	0.260	0.001	−0.286	4.498

II. Strain effect on band structures.

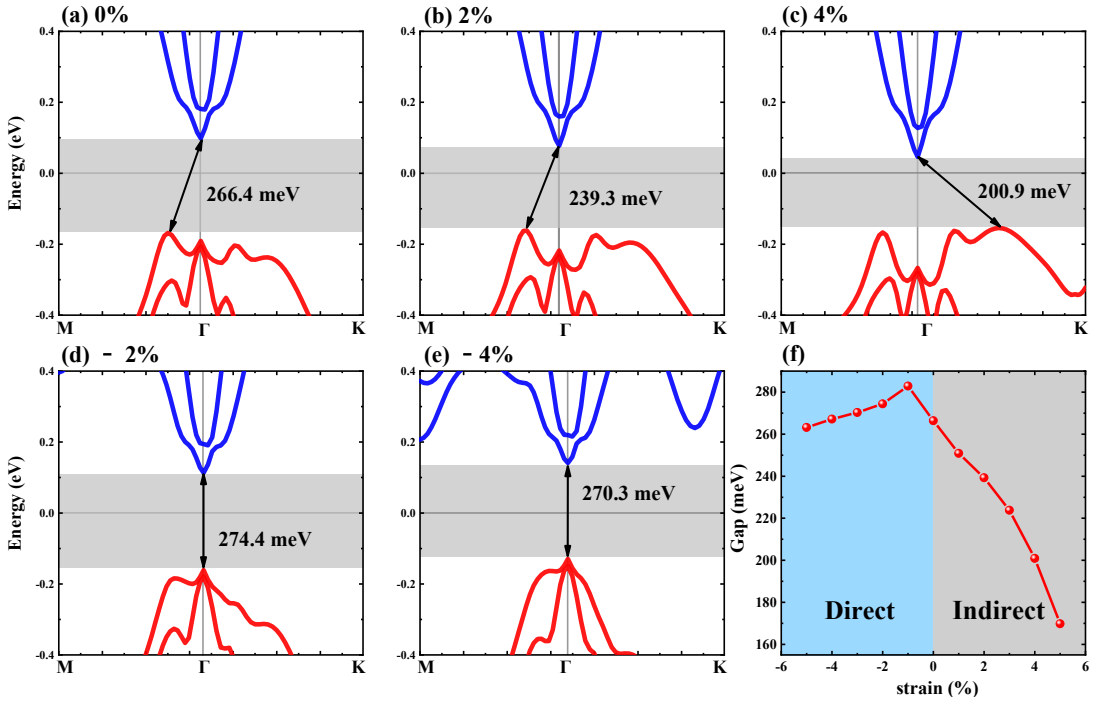

Fig. S3. (a)~(e) Band structures of Janus MSBST monolayer under different biaxial strain ε with M//*x*. (f) The band gap of Janus MSBST as a function of strain ε. Blue and red markers represent Sb-*p* and Te-*p* orbitals, respectively. The Fermi levels are set to be zero.

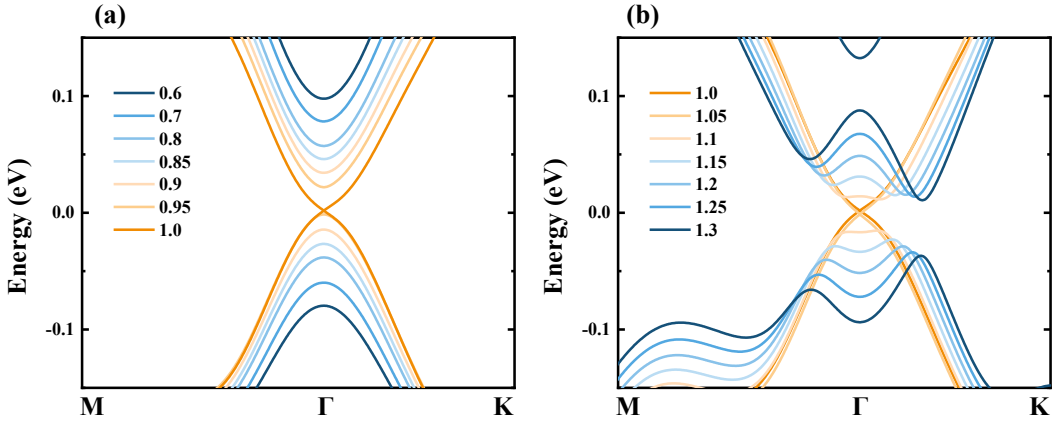

Fig. S4. Band structures of Janus MSBST monolayer under different strengths of spin-orbital coupling (SOC).

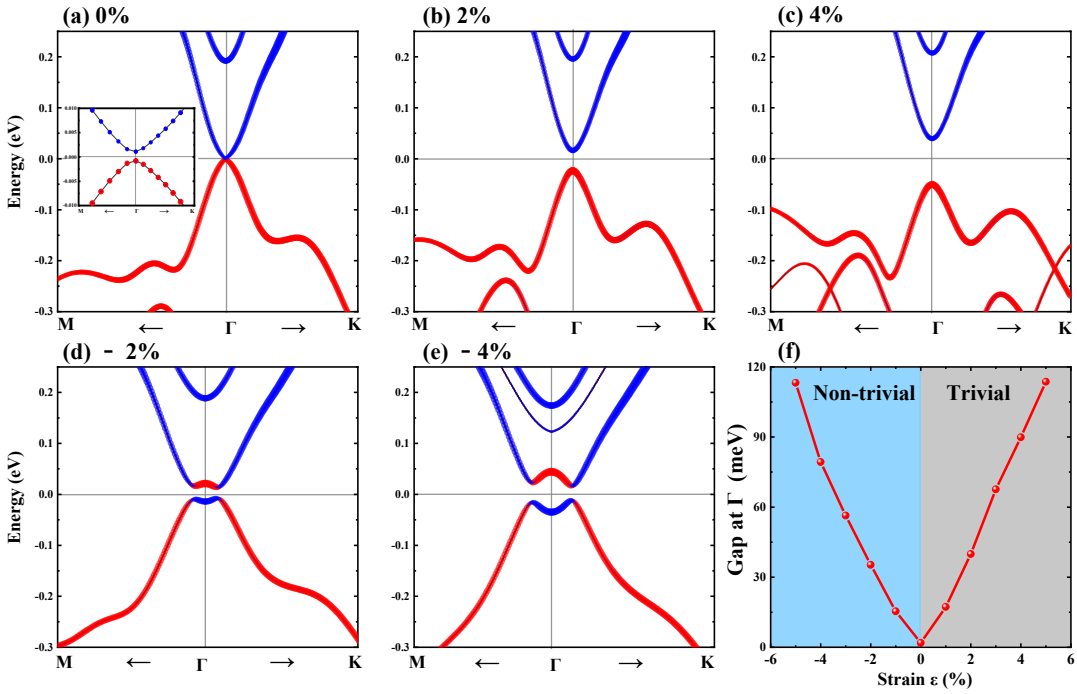

Fig. S5. (a)~(e) Band structures of Janus MSBST monolayer under different biaxial strain ε with M//z. (f) The band gap of Janus MSBST as a function of strain ε. Blue and red markers represent Sb-*p* and Te-*p* orbitals, respectively. The Fermi levels are set to be zero.

III. Tight binding (TB) model

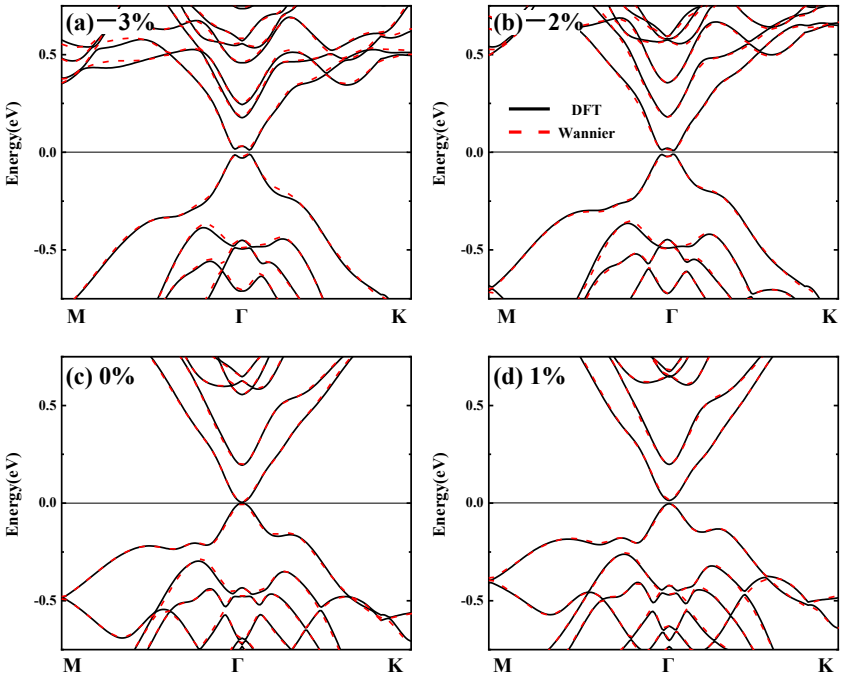

Fig. S6. Wannier interpolated band structures of Janus MSBST under different strain ε. Black solid lines: the band structures from DFT calculations. Red dash lines: the Wannier interpolated band structures. The Fermi levels are set to zero.

IV. Monte Carlo (MC) and Micromagnetic simulations

In order to eliminate the potential error caused by finite-size effects, we applied the periodic boundary conditions in our MC simulation, and then the Binder Cumulant of Janus MSBST with different lattice sizes have been investigated. Also, we plot the MC simulations of magnetic moment and susceptibility curves for Janus MSBST under different strains in Fig. S7.

It can be seen that T_C is nearly unchanged when L is greater than 36 in Fig. S7(a). Moreover, from Fig. S7(b), one can find that when L → ∞, the estimate T_C is about 12K, which might be smoothly extrapolated to the thermodynamic limit. In addition, to obtain reliable simulated data with high accuracy, a 40×40×1 supercell was adopted in our MC simulation. We started with ferromagnetic configurations and used 5×10^4 sweeps to sufficiently thermalize the system into equilibrium at each temperature site, and the next 6×10^4 sweeps per site for acquiring the statistical results.

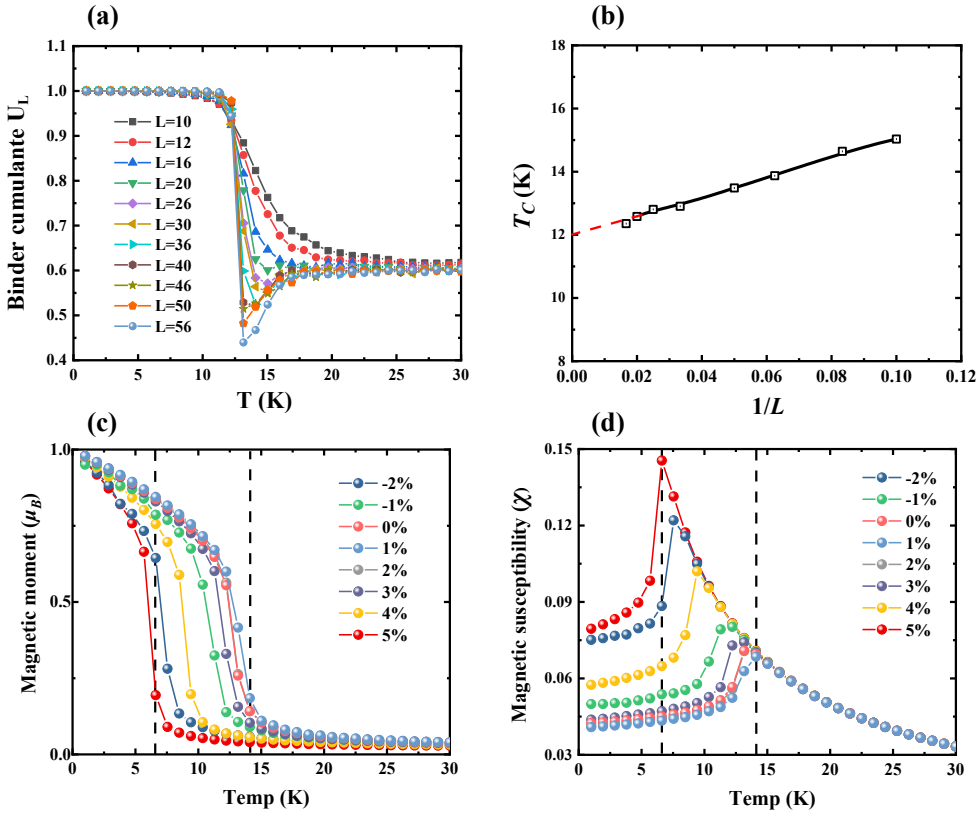

Fig. S7. (a) The Binder cumulants (U_L) of Janus MSBST as a function of temperature with clusters of various sizes L. (b) The plot of Curie temperature T_C as a function of 1/L. The Binder cumulants and T_C are obtained using the anisotropic Heisenberg model on full periodic boundary conditions. MC simulations of (c) magnetic moment and (d) susceptibility as functions of temperature for Janus monolayer MSBST with different strain.

The micromagnetic simulation were calculated by the frame of the Vampire package. We redefine the lattice direction to convert the rhombohedral unit cell [Fig. S1(c)] to a rectangular lattice, which contains 18 magnetic Mn atoms with a =12.36 Å and b = 21.42 Å, as shown in Fig. S8. Then, a 28×16×1 super cell based on this rectangular lattice (which is about 350 Å × 350 Å) with periodic boundary conditions were used to perform spin texture under external magnetic field.

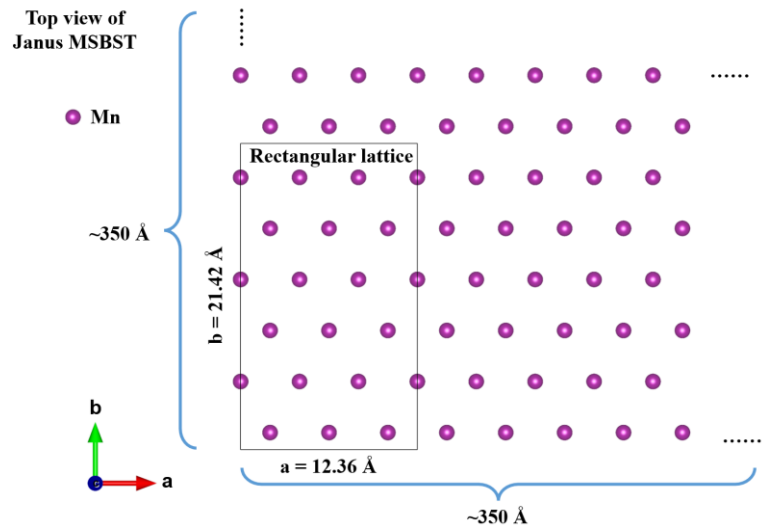

Fig. S8. The schematic of rectangular lattice and super cell used in micromagnetic simulation.

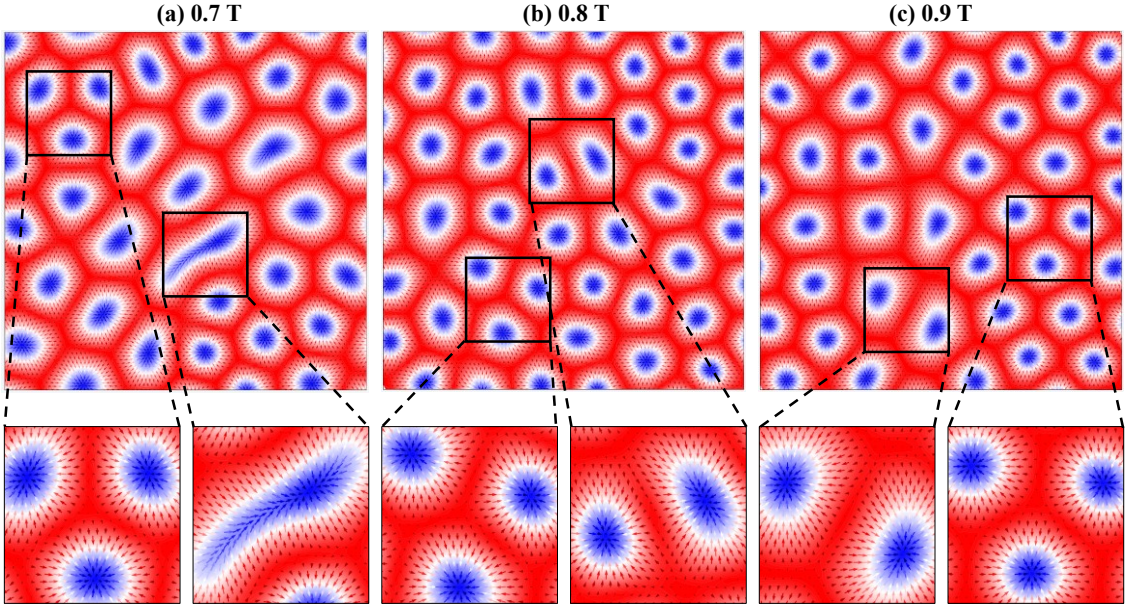

Fig. S9. Spin textures of unstrained MSBST at magnetic field of (a) 0.7 T, (b) 0.8 T and (c) 0.9 T. The lower panel shows the enlarged view of the black box in the upper panel, with arrows indicating the direction of spin. The simulation area in the upper panel is 400×400 $Å^2$.

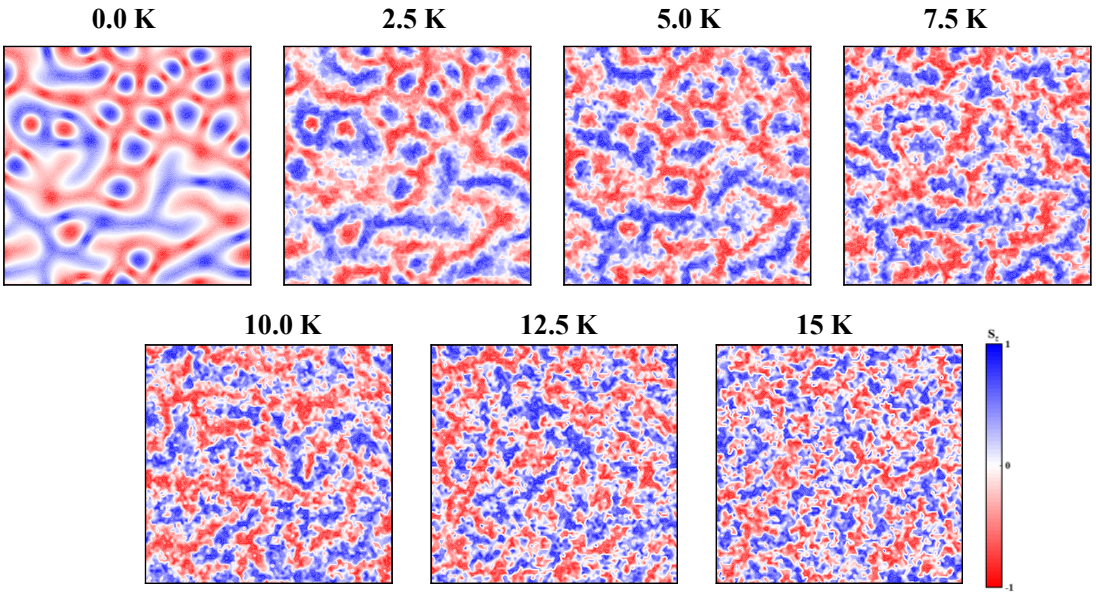

Fig. S10. Evolution of spin texture of Janus MSBST at 0% strain under different temperatures.

Reference

1. M. M. Otrokov, Klimovskikh, II, H. Bentmann *et al.*, Prediction and observation of an antiferromagnetic topological insulator. *Nature* **576**, 416-422 (2019).
2. M. M. Otrokov, I. P. Rusinov, M. Blanco-Rey *et al.*, Unique Thickness-Dependent Properties of the van der Waals Interlayer Antiferromagnet $MnBi_2Te_4$ Films. *Phys. Rev. Lett.* **122**, 107202 (2019).
3. F. Xue, Z. Wang, Y. Hou *et al.*, Control of magnetic properties of $MnBi_2Te_4$ using a van der Waals ferroelectric III_2-VI_3 film and biaxial strain. *Phys. Rev. B* **101**, 184426 (2020).
4. T. Zhu, A. J. Bishop, T. Zhou *et al.*, Synthesis, Magnetic Properties, and Electronic Structure of Magnetic Topological Insulator MnBi2Se4. *Nano Lett* **21**, 5083-5090 (2021).